Hemodynamic and electrophysiological signals of conflict processing in the Chinese-character Stroop task: a simultaneous near-infrared spectroscopy and event-related potential study

Jiahuan Zhai
Ting Li
Zhongxing Zhang
Hui Gong
Huazhong University of Science and Technology
Wuhan National Laboratory for Optoelectronics
Britton Chance Center for Biomedical Photonics
1037 Luoyu Road
Wuhan 430074
China

Abstract. A dual-modality method combining continuous-wave near-infrared spectroscopy (NIRS) and event-related potentials (ERPs) was developed for the Chinese-character color-word Stroop task, which included congruent, incongruent, and neutral stimuli. Sixteen native Chinese speakers participated in this study. Hemodynamic and electrophysiological signals in the prefrontal cortex (PFC) were monitored simultaneously by NIRS and ERP. The hemodynamic signals were represented by relative changes in oxy-, deoxy-, and total hemoglobin concentration, whereas the electrophysiological signals were characterized by the parameters P450, N500, and P600. Both types of signals measured at four regions of the PFC were analyzed and compared spatially and temporally among the three different stimuli. We found that P600 signals correlated significantly with the hemodynamic parameters, suggesting that the PFC executes conflict-solving function. Additionally, we observed that the change in deoxy-Hb concentration showed higher sensitivity in response to the Stroop task than other hemodynamic signals. Correlation between NIRS and ERP signals revealed that the vascular response reflects the cumulative effect of neural activities. Taken together, our findings demonstrate that this new dual-modality method is a useful approach to obtaining more information during cognitive and physiological studies. [DOI: 10.1117/1.3247152]

Keywords: Chinese characters; Stroop task; near-infrared spectroscopy; event-related potential; prefrontal cortex.

Paper 09015RR received Jan. 15, 2009; revised manuscript received Aug. 2, 2009; accepted for publication Aug. 4, 2009; published online Oct. 29, 2009.

1 Introduction

Conflict processing, which includes conflict monitoring and solving, is necessary to accomplish a specific task in a complex situation. This processing typically occurs when a stimulus is accompanied by interference or facilitation information. The Stroop task is a classical method of studying conflict processing,[1,2] which was developed in 1935 by John Ridley Stroop, who discovered a cognitive delay when the meaning of a printed word was inconsistent with the color of the word. This phenomenon was dubbed the Stroop effect.[3] The main feature of the Stroop paradigm is instructing the subject to respond to one dimension of a stimulus while ignoring its other dimensions, including interference and facilitation between different dimensions. Because the Stroop effect reflects conflicts between different pieces of information,[4] it has been widely used in both clinical neuropsychology and experimental psychology.[5,6] Additionally, the task is often considered a gold standard in studies of attention.[7] Many researchers have also evaluated the cognitive control abilities of patients with disorders using Stroop or Stroop-like tests.

Studies measuring neural electrical activity have shown that responses to the Stroop task consist of two steps: stimulus evaluation processing and response production processing, which is also known as conflict processing. The response originates in the conflict processing[8,9] and event-related potential (ERP) components, represents different cognitive courses, and appears after 350 ms.[10–12] This implies that the generator of these components is located at the area executing the cognitive function. Other studies measuring hemodynamic signals and other metabolic changes showed that the anterior cingulate cortex (ACC), prefrontal cortex (PFC), and temporo-parietal cortex were activated during the Stroop task.[13,14] Among these brain regions, the ACC and PFC, which are essential for goal-directed behavior with top-down control,[15] play a central role in the Stroop effect.[10,12,16] In particular, the PFC implements cognitive conflict control in response production processing.[17,18]

Address all correspondence to: Hui Gong, Britton Chance Center for Biomedical Photonics, Wuhan National Laboratory for Optoelectronics, Huazhong University of Science and Technology, Wuhan 430074, China; Tel: +86-27-8779-2033; Fax: +86-27-8779-2034; E-mail: huigong@mail.hust.edu.cn

1083-3668/2009/14(5)/054022/7/$25.00 © 2009 SPIE

Near-infrared spectroscopy (NIRS) is a noninvasive optical method that takes advantage of the sensitivity of NIR light to hemoglobin oxygenation-state shifts.[19–21] Since Chance et al.[22] proved that hemodynamic signals in the brain could be quantified by NIRS, many studies have demonstrated the validity of this method[20,23–27]. In comparison to functional magnetic resonance imaging, NIRS can measure changes in blood volume, oxy-hemoglobin (Δ[oxy-Hb]), deoxy-hemoglobin (Δ[deoxy-Hb]), and cytochrome-oxidase redox state.[25] In most cases, Δ[oxy-Hb], Δ[deoxy-Hb], and total-hemoglobin (Δ[tot-Hb], the sum of Δ[oxy-Hb] and Δ[deoxy-Hb]) act as NIRS parameters that vary with brain cognitive activity.[25,28] One method, known as continuous-wave NIRS (CW-NIRS), does not require strict motion restriction and is thus well suited to studying children and the elderly.[29] Moreover, the CW-NIRS system is portable and inexpensive[30] and may potentially be coupled with ERP.[31,32] Thus, CW-NIRS is a promising technique with many possible clinical applications.

Meanwhile, ERP measurements detect electrophysiological signals using scalp electrodes. Although an ERP signal has good temporal resolution, its spatial resolution is relatively poor.[31] In cognitive psychology, identifying time courses with ERP components is a common technique because the ERP signal supplements information about the time course of cognitive processes.

The hemodynamic signal reflects oxygenation, whereas the electrophysiological signal reflects neural network activity. Together, these two signals provide a physiological index of brain activation. Simultaneous measurement of hemodynamic and electrophysiological signals may improve understanding of neural mechanisms and the coupling of vascular and neural responses. Whereas conventional monitoring methods only measure one of the signals, recent research has shown that dual-modality approaches, combining two or more measurement techniques, are both advantageous and feasible.[31,33–35]

In this study, we report a dual-modality method combining CW-NIRS and ERP measurements to monitor hemodynamic and electrophysiological signals, simultaneously, at four PFC regions. To better understand the role of the PFC in conflict processing, a Chinese-character color-word Stroop task, including congruent, incongruent, and neutral stimuli, was used to study neural activity and its coupling with vascular responses.

2 Methods

2.1 *Subjects*

Sixteen healthy volunteers (right-handed, native Chinese speakers, age 21–23 years old, 6 females and 10 males) participated in this experiment. All subjects had normal or corrected-to-normal vision and normal color vision. No subject had a history of neurological, medical, or psychiatric disorders, and none was taking medication during the measurement period. Before the formal experiment, consent was obtained from each volunteer, and a practice exercise was arranged to familiarize subjects with the task.

2.2 *Stimuli and Procedure*

An event-related Stroop task was designed for this study. The stimuli consisted of two Chinese characters, and subjects were instructed to decide whether the color of the upper one matched the meaning of the lower one.[13] If the answer was "Yes," subjects pressed the F button with the index finger of their left hand, whereas if the answer was "No," they pressed the J button with the index finger of their right hand.

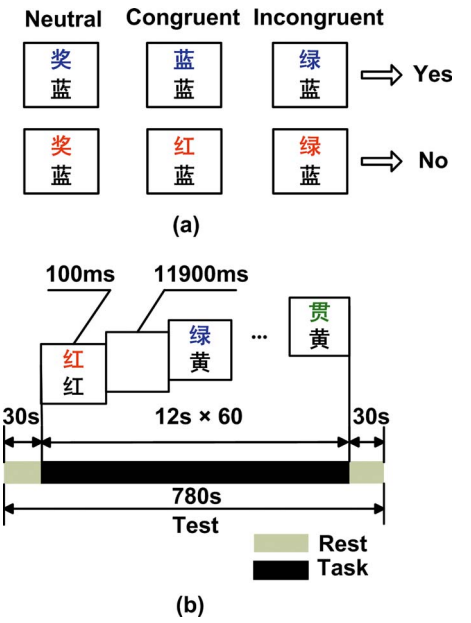

Fig. 1 Experimental design. (a) Stimulus design of each trial, including congruent, incongruent, and neutral stimuli. Each subject was asked whether the color of the upper character was consistent with the meaning of lower character. The correct answer was "Yes" for the three pictures in the upper row and "No" for the three pictures in the lower row. 貫, 獎 mean "pass though" and "prize," respectively. 红, 綠, 黃, 蓝 correspond to "red," "green," "yellow," and "blue." (b) Test protocol: between 30-s rests, 60 trials are administered in a pseudo-random sequence. Each stimulus is displayed for only 100 ms, and each trial lasts 12 s total. (Color online only.)

Three kinds of stimuli were displayed [Fig. 1(a)]: congruent, incongruent, and neutral. These all included lower color-meaning characters in black font. In the congruent trial, the upper character was a color-meaning word (红, 綠, 黃, 蓝 meaning "red," "green," "yellow," and "blue") for which the color and meaning were consistent. In the incongruent trial, the upper character was a color-meaning word with disparate color and meaning. Meanwhile, in the neutral trial, the upper character was a non-color-meaning word (貫, 獎, 球, 涂, meaning "pass through," "prize," "ball," and "print"). The test included 60 judgment trials (20 congruent, 20 incongruent, and 20 neutral stimuli). In half of the trials, the color of the upper character matched that of the lower character, whereas the two characters were unmatched in the remaining half of the trials

The experimental procedure was as follows [Fig. 1(b)]. A white cross appeared in the center of the screen for 30 s, and the subjects should rest. A chime sounded right before the first stimulus appeared, commencing the 60 trials. During the trials, each picture remained on the screen for, followed by an empty screen for 11,900 ms. The order of stimuli was pseudorandom. After the final trial ended, the white cross again appeared for 30 s, indicating a rest period.

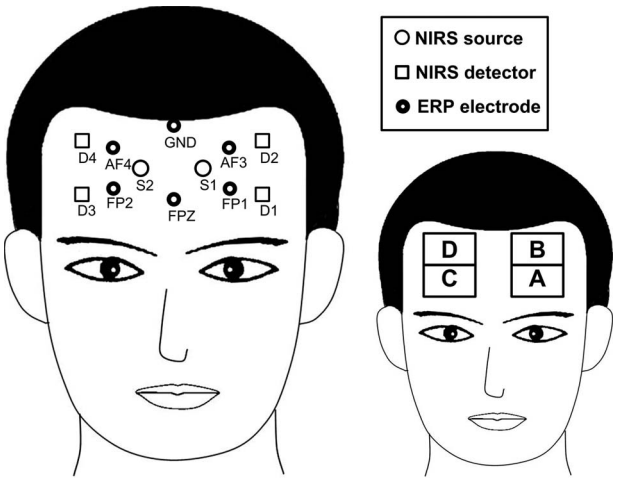

Fig. 2 Probe locations and defined area. (a) locations of NIRS optodes and ERP electrodes. (b) area defined for four channels. Channel A contains electrode FP1 of ERP and the Source 1-Detector 1 pair of NIRS; channel B contains electrode AF3 of ERP and the Source 1-Detector 2 pair of NIRS; channel C contains electrode FP2 of ERP and the Source 2-Detector 3 pair of NIRS; and channel D contains electrode AF4 of ERP and the Source 2-Detector 4 pair of NIRS.

2.3 *NIRS*

The CW-NIRS instrument used to measure changes in oxy-, deoxy-, and tot-hemoglobin concentration is a portable brain function imager operating at three wavelengths (735, 805, and 850 nm). It includes a probe, a measuring and controlling module, and a personal computer.[36] The probe has two sources and four detectors that define four areas. As shown in Fig. 2, channel A corresponds to the inferior left PFC, B corresponds to the superior left PFC, C corresponds to the inferior right PFC, and D corresponds to the superior right PFC. The sampling frequency is 3.3 Hz, and the separation of source-detector pair is 4 cm, which makes the light available to penetrate the scalp, skull, and cerebrospinal fluid, and be modulated by cortical activity.[37]

The raw data were bandpass filtered using a Hanning Window with a cutoff frequency of 0.01 Hz to remove the baseline drifts and 0.7 Hz to filter pulsations due to heartbeat and other physiological noise. Three parameters were analyzed: the average amplitude, peak amplitude, and latency of the peak amplitude of each trial. We assessed 36 combinations based on three stimuli (congruent, incongruent, and neutral), three hemodynamic parameters (oxy-, deoxy-, and tot-Hb) and four channels (A–D). The average amplitude of each stimulus condition was averaged across 20 trials per subject. The oxy-Hb and tot-Hb maxima and deoxy-Hb minimum were considered the peak amplitudes of each trial.

2.4 *ERP*

The electrophysiological signal was recorded by a 64-channel system using a bandpass filter of 0.05–100 Hz and sampling rate of 1000 Hz (SynAmps[2] amplifiers, Neuroscan Ltd.). Only four electrodes (FP1, FP2, AF3, and AF4 of 64 scalp sites standardized by the American Electroencephalographic Society) located on the PFC were used in the study and symmetrically distributed from the NIRS optodes (Fig. 2). The reference electrodes were placed on the bilateral mastoid bone behind the ear. An electrooculogram was also recorded by four electrodes placed around the eyes. The impedance of all electrodes was <5 kΩ during recording.

The ERP data were processed offline using Scan4.3 software (Neuroscan Ltd.). For each subject, the ocular artifact was first removed. Next, the data were arranged into epochs (200 ms prestimulus to 1000 ms poststimulus), baseline corrected, averaged with other data originating from the same kind of stimuli, filtered by finite impulse response (FIR) (0.8–17 Hz, 24 dB/oct, zero phase shift), and baseline corrected again. All subjects' data were then group averaged.

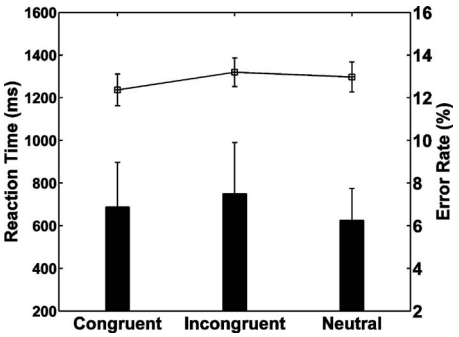

Fig. 3 Reaction time (line) and error rate (bar) averaged across all subjects. Mean ± SEM (standard error of measurement).

2.5 *NIRS-ERP Synchronization and Comparison*

Presentation 0.53 software emitted signals to trigger NIRS and ERP sampling at the beginning of the test. The NIRS-ERP synchronization error was much smaller than the NIRS sampling interval. Both correlations and linear regression were utilized to compare the NIRS and ERP signals. No correction for multiple comparisons was performed, and results were considered significant if $p<0.05$.

3 Results

3.1 *Behavioral Data*

As shown in Fig. 3, the mean reaction time for the incongruent stimulus (1319.65 ± 67.14 ms) was longer than that for the congruent (1236.91 ± 74.08 ms) or neutral stimulus (1297.47 ± 70.34 ms). Repeated measure analysis of variance (ANOVA) indicated statistically significant differences between the incongruent stimulus and the other two stimuli (congruent versus incongruent $F_{1,15}=7.081$, $P=0.018<0.05$; congruent versus neutral $F_{1,15}=1.795$, $P=0.200>0.05$; incongruent versus neutral $F_{1,15}=5.212$, $P=0.037<0.05$). The mean error rate was higher for the incongruent stimulus ($7.5 \pm 2.4\%$) than for the congruent ($6.9 \pm 2.1\%$) or neutral stimuli ($6.25 \pm 1.5\%$). Error rate had no significant effect for all three stimuli by repeated-measure ANOVA ($F_{2,30}=0.211$, $P>0.05$). The relative degrees of error rate for the three stimuli were also similar. However, the between-subjects effect was significant and the variance of each combination was large in magnitude.

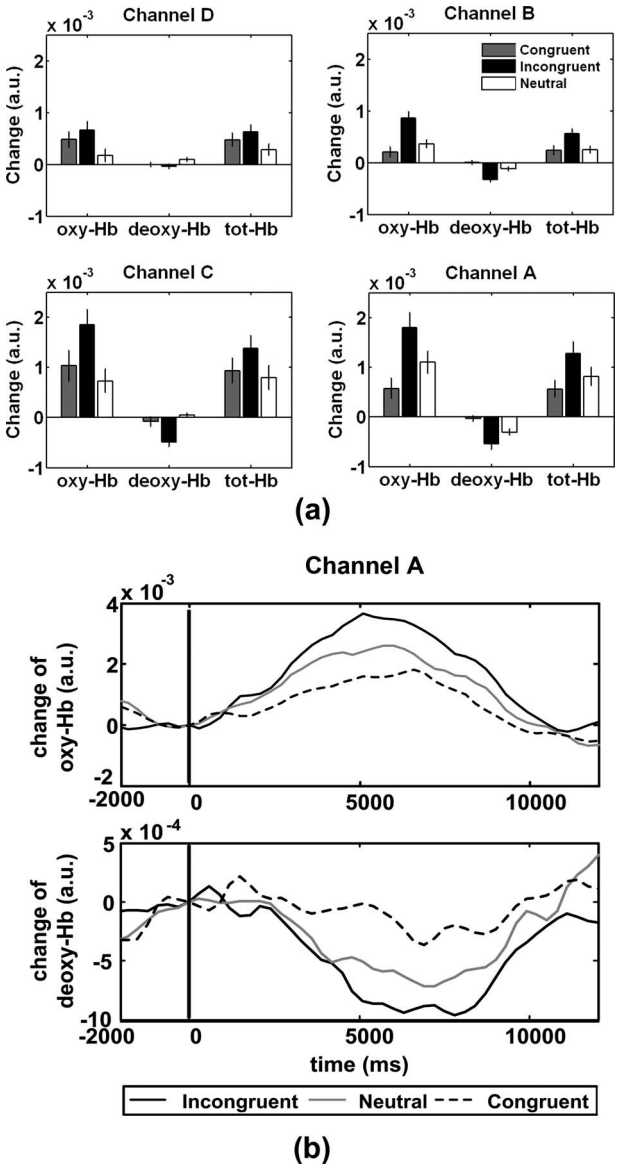

Fig. 4 Hemodynamic signal measured by NIRS. (a) Average amplitudes of Δ[oxy-Hb], Δ[deoxy-Hb], and Δ[tot-Hb] detected by NIRS. Each value is an average of all changes at the same location and for the same trial around all subjects. Four channels are defined as in Fig. 2. Mean±SEM. (b) Time courses of the averaged Δ[oxy-Hb] and Δ[deoxy-Hb] in channel A (left inferior area). The time period extends from 2 s prestimulus to 12 s post-stimulus, and the gray bar represents the 100-ms stimulus-displaying period.

3.2 *NIRS data*

As shown in Figure 4(a), the average amplitudes of Δ[oxy-Hb] and Δ[deoxy-Hb] after an incongruent stimulus were significantly larger than those resulting from the other two stimuli (Δ[oxy-Hb]: congruent versus incongruent $F_{1,63}=6.947$, $P=0.011<0.05$; incongruent versus neutral $F_{1,63}=6.749$, $P=0.012<0.05$; Δ[deoxy-Hb]: congruent versus incongruent $F_{1,63}=5.436$, $P=0.023<0.05$; incongruent versus neutral $F_{1,63}=5.216$, $P=0.026<0.05$). The activation of congruent and neutral stimuli were not significantly different from each other (Δ[oxy-Hb]: $F_{1,63}=0.008$, $P=0.928>0.05$). Compared to the superior PFC (channels B and D), the inferior PFC (channels A and C) had a higher signal amplitude (Δ[oxy-Hb]: $F_{1,95}=26.201$, $P=0.000<0.05$). In addition, note that the amplitude change of Δ[oxy-Hb] was larger than Δ[deoxy-Hb] in all channels and the amplitude of Δ[tot-Hb] was similar to that of Δ[oxy-Hb].

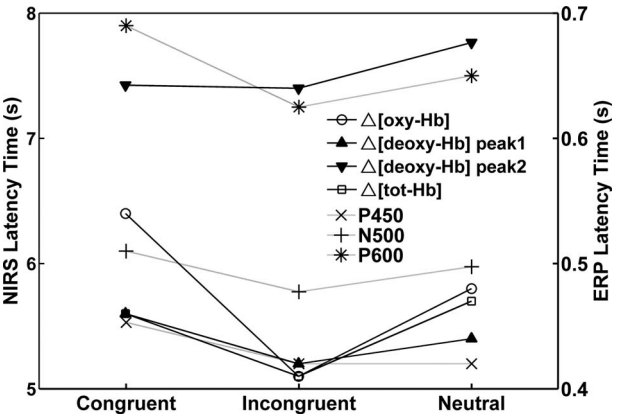

Fig. 5 Latency time of NIRS and ERP measurements averaged across all subjects and channels. The NIRS signal includes four parameters because Δ[deoxy-Hb] has two peaks in each channel (Δ[deoxy-Hb] peak 1 and Δ[deoxy-Hb] peak 2). The ERP signal includes P450, N500, and P600 as its three parameters. To more clearly display the average values, the error bar was omitted.

Figure 4(b) shows the amplitude of Δ[oxy-Hb] and Δ[deoxy-Hb] during a trial in the left inferior area (channel A). The response to incongruent stimuli occurred more rapidly, and its decrease occurred later, than that of congruent or neutral stimuli. The time courses of both Δ[oxy-Hb] and Δ[deoxy-Hb] also showed that the incongruent stimulus had the largest hemodynamic response, which returned to baseline after ~11 s poststimulus (1 s before the next stimulus).

The time course of Δ[deoxy-Hb] showed two small peaks for all stimuli. However, repeated-measure ANOVA showed no significant difference between these two peaks for all three stimuli. The time courses of both Δ[oxy-Hb] and Δ[tot-Hb] had two peaks only in channel B after congruent and neutral stimuli; in this study, we only chose the second peak for data analysis.

The first peak latency of Δ[deoxy-Hb] was between 5 and 6 s, and the second was between 7 and 8 s. The only peak latency of Δ[oxy-Hb] and Δ[tot-Hb] was between 5 and 7 s, between the first and second peak latencies of Δ[deoxy-Hb], except for that of the incongruent stimulus. The incongruent stimulus, which was the most challenging, had the shortest latency time (Δ[oxy-Hb]: congruent versus incongruent $F_{1,15}=5.757$, $P=0.030<0.05$; incongruent versus neutral $F_{1,15}=9.001$, $P=0.009<0.01$; Δ[deoxy-Hb] peak 1: congruent versus incongruent $F_{1,15}=14.087$, $P=0.002<0.01$; incongruent versus neutral $F_{1,15}=4.879$, $P=0.043<0.05$; Δ[deoxy-Hb] peak 2: congruent versus incongruent $F_{1,15}=12.093$, $P=0.003<0.01$; incongruent versus neutral $F_{1,15}=4.825$, $P=0.044<0.05$; see Fig. 5).

3.3 *ERP Data*

On the basis of ERP data, three feature-based components, P450 (positive component from 400–450 ms time window),

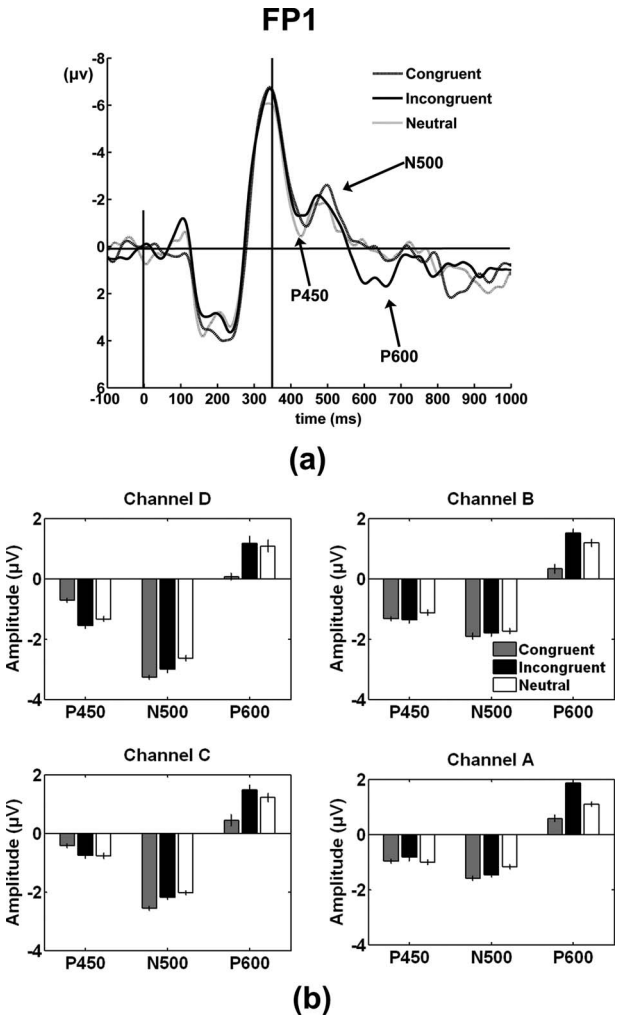

Fig. 6 (a) Electrophysiological signal in FP1 (channel A). The first vertical line labels the start of the stimulus, and the second vertical line labels the 350 ms after stimulation. The three components of P450, N500, and P600 marked by arrows show significant differences between different stimuli after 350 ms. (b) Average amplitude of three components from ERP measurement. Each value is an average of the related component at the same location and for the same trial around all subjects. Mean±SEM.

N500 (negative component from 450–550 ms time window), and P600 (positive component from 600–700 ms time window), showed significant differences for different stimuli. As shown in Fig. 6(a), all stimulation responses appeared later than 350 ms. There were 36 combinations resulting from the combination of the three stimuli, three feature components and four channels.

Figure 6(b) shows the components' amplitude in the channels. The activation level displayed by P600 corresponded to the difficulty level of the stimulus (incongruent > neutral > congruent; congruent versus incongruent $F_{1,63}=9.176$, $P=0.004<0.01$; incongruent versus neutral $F_{1,63}=6.607$, $P=0.013<0.05$; congruent versus neutral $F_{1,63}=5.752$, $P=0.019<0.05$). However, N500's amplitude for the congruent stimulus was the largest (congruent versus incongruent $F_{1,63}=9.176$, $P=0.004<0.01$; incongruent versus neutral $F_{1,63}=7.965$, $P=0.006<0.01$). P600 had the strongest response at the left inferior PFC (channel A), whereas N500's strongest response was in the right superior area (channel D). For P450, the incongruent stimulus elicited a larger-amplitude response in the superior PFC but a smaller response in the inferior area. The peak latency of ERP also showed that more difficult stimuli resulted in shorter latency time.

3.4 *NIRS-ERP Correlation*

To evaluate the correlation between the NIRS and ERP signals, we compared peak latency and peak amplitude data. We first used Pearson correlation analysis to find stronger correlation parameter pairs and then used a linear regression model to characterize the magnitude of the correlation for those pairs. On the basis of the peak latency data, we calculated significant correlations between Δ[oxy-Hb] and N500 ($r=0.718$, $P<0.01$) and between Δ[oxy-Hb] and P600 ($r=0.744$, $P<0.01$). Meanwhile, P450 had no significant correlation with any hemodynamic parameter. In addition, the single latency peak of Δ[deoxy-Hb] did not correlate with electrophysiological signals. Analysis using a linear regression model demonstrated good linearity for latencies of N500 and P600 and Δ[oxy-Hb] ($R^2=0.636$, $P=0.011$). The model also revealed very good linearity for latencies of N500 and P600 and both peak latencies of Δ[deoxy-Hb] ($R^2=0.868$, $P=0.012$). When the P450 latency was added as another independent variable, better linearity was achieved (Δ[oxy-Hb]: $R^2=0.651$, $P=0.031$; Δ[deoxy-Hb]: $R^2=0.932$, $P=0.013$).

The peak amplitude of P600 significantly correlated with the amplitudes of many hemodynamic parameters, especially in the inferior left area (Table 1). A 0.05-level correlation between P600 and the second peak of Δ[deoxy-Hb] was observed, but not between P600 and the first peak. In contrast to P600, no significant correlation was observed between N500 or P450 and any hemodynamic parameter. A linear regression model was established using the peak values of N500, P600, and the first peak value of Δ[deoxy-Hb] as independent variables and the second peak value of Δ[deoxy-Hb] as a dependent variable ($R^2=0.791$, $P=0.018$). A better linear regression model was also established with P450 as an additional independent variable ($R^2=0.868$, $P=0.003$). Thus, a model with more component information had better linearity, just as in the case of the peak latencies. Meanwhile, the peak value of Δ[oxy-Hb] had no significant linear relationship with electrophysiological signals.

4 Discussion and Conclusions

In this study, all behavioral, NIRS, and ERP data reflected the Stroop effect. Both hemodynamic and electrophysiological signals, measured simultaneously by NIRS and ERP, respectively, at four regions of the PFC (channels A–D) were consistent with corresponding independent measurements. The experimental results demonstrated the feasibility of using a dual-modality method, combining CW-NIRS and ERP measurements, for investigating cognition and physiology.

4.1 *PFC Activation in Conflict Solving Processing*

As mentioned earlier, responses to the Stroop task usually include two-step stimulus evaluation processing and response production processing (also known as conflict processing). Al-

Table 1 Correlation of NIRS and ERP signal amplitudes (Pearson correlation, $N=12$).

	oxy-Hb peak	deoxy-Hb peak 1	deoxy-Hb peak 2	oxy-Hb mean	deoxy-Hb mean
P600	0.59[a]	−0.56	−0.683[a]	0.583[a]	−0.776[b]
N500	0.349	−0.294	−0.537	0.291	−0.453
P450	0.502	−0.345	−0.213	0.308	−0.193

The tot-Hb data are not shown because the correlations related to tot-Hb were the same as that of oxy-Hb. Also, note that "deoxy-Hb 1" and "deoxy-Hb 2" correspond to the two peak values.

[a]Correlation is significant at the 0.05 level (2-tailed).

[b]Correlation is significant at the 0.01 level (2-tailed).

though the hemodynamic signals measured by NIRS provided good PFC location information, they could not resolve or distinguish whether the step occurred in the PFC due to the Stroop effect. Meanwhile, ERPs directly reflect neural activity and the component latency is consistent with the sequence of cognitive activity.

Compared to previous studies of the Stroop effect, stimulated using either English words[12] or Chinese characters,[38] our ERP data showed similar time courses that also suggested that conflict processing happens in the PFC. On the basis of these data, the three feature-based components P450, P600, and N500 showed significant correlation with the Stroop effect. We also found significant spatial and temporal correlations between P600 and hemodynamic signals, whereas N500 and P450 did not show significant spatial correlation. Considering that ERP data have higher temporal resolution but lower spatial resolution than NIRS data, the generators of N500 and P450 are located farther from the PFC than that of P600. P600 shows the most significant correlation with the left inferior area, suggesting that its generator is proximal to this area. The larger amplitude of hemodynamic and electrophysiological signals in the left inferior area also supports this inference.

P600 is the last component of ERP, representing the final course of cognitive neutral activity (Fig. 6). In the Stroop task, the final course of cognition is solving conflict and receiving judgment. The results of our study support the hypothesis that conflict solving is one function of the PFC and that the PFC is the last activation area in the Stroop task. N500 is slightly earlier, possibly reflecting conflict monitoring processing. Some researchers have reported that the ACC is activated after the PFC,[10,38] whereas others have shown that the ACC plays a role in conflict monitoring,[39–42] implying that it is activated earlier than the PFC. Our study supports the former finding.

4.2 *Physiological Signals in Conflict Solving Processing*

The results of our linear regression model suggest that hemodynamic signals reflect the cumulative effect of electrophysiological signals. However, the contribution of each electrophysiological component to the peak hemodynamic signal is different. For example, our data show that the contribution of P450 is not as substantial as that of P600, suggesting that hemodynamic change mainly reflects conflict solving processing. The linear regression models of peak amplitude imply the cumulative effect directly. The models of latency time similarly imply a cumulative effect, although the peak amplitude of the hemodynamic signal appears later than that of electrophysiological components.

As shown in Sec. 3.2, the measured time course of the hemodynamic signals included two peaks. However, a previous study with a similarly event-related design reported only one peak.[13] This discrepancy may be because the previous study's NIRS signal was fit to a Gaussian function. Additionally, the study's behavioral data differed from those of the current report, in which the reaction time was >1 s for all subjects. The difference in reaction time is related to the response bias of the subject and experimental instructions. Longer reaction time may cause divided peaks.

Our results also demonstrate that Δ[deoxy-Hb] is a more sensitive parameter that strongly correlates with electrophysiological signals. Δ[Deoxy-Hb] reflects oxygen consumption due to active cognition, so its two peaks imply the occurrence of two cognitive processes. It is suggested that the hemodynamic parameters, in addition to electrophysiological signal, can provide comprehensive information for dissociating cognitive processes.

In conclusion, we investigated the correlation between hemodynamic and electrophysiological signals in the Chinese-character Stroop paradigm using a dual-modality (NIRS and ERP measurements) approach. The positive component from 600 to 700 ms showed strong correlation with the hemodynamic parameters in the PFC. On the basis of correlation analysis of NIRS and ERP signals, the PFC executes conflict solving. The hemodynamic signal reflects the cumulative effect of the neural response. Δ[Deoxy-Hb] had two peaks during the trial and was more sensitive than other hemodynamic parameters. Supplementing NIRS with ERP's temporal data allows NIRS to identify the specialization function of an area and reveal, cognitive connections between areas. Thus, this dual-modality method is a promising approach to investigating neurovascular coupling in physiology and cognition.

Acknowledgments

This research was supported by the Program for Changjiang Scholars and Innovative Research Team in the University, the 111 projects, and the Ph.D. Programs Foundation of the Ministry of Education of China (Grant No. 20070487058). We thank all subjects for their participation.

References

1. S. Zysset, K. Muller, G. Lohmann, and D. Y. von Cramon, "Color-word matching stroop task: separating interference and response conflict," *Neuroimage* **13**(1), 29–36 (2001).
2. R. C. Kadosh, K. C. Kadosh, A. Henik, and D. E. J. Linden, "Processing conflicting information: facilitation, interference, and functional connectivity," *Neuropsychologia* **46**(12), 2872–2879 (2008).
3. J. R. Stroop, "Studies of interference in serial verbal reactions," *J. Exp. Psychol.* **18**, 643–662 (1935).
4. C. M. Macleod and K. Dunbar, "Training and Stroop-like interference: evidence for a continuum of automaticity," *J. Exp. Psychol.* **14**(1), 126–135 (1988).
5. C. M. Macleod, "Half a century of research on the Stroop effect: an integrative review," *Psychol. Bull.* **109**(2), 163–203 (1991).
6. D. T. Stuss, D. Floden, M. P. Alexander, B. Levine, and D. Katz, "Stroop performance in focal lesion patients: dissociation of processes and frontal lobe lesion location," *Neuropsychologia* **39**(8), 771–786 (2001).
7. C. M. Macleod, "The Stroop task: the 'Gold Standard' of attentional measures," *J. Exp. Psychol.* **121**, 12–15 (1992).
8. A. B. Ilan and J. Polich, "P300 and response time from a manual Stroop task," *Clin. Neurophysiol.* **110**, 367–373 (1999).
9. J. Grapperon, F. Vidal, and P. Leni, "Contribution of event-related potentials to the knowledge of the Stroop test mechanisms," *Neurophysiol. Clin.* **28**(3), 207–220 (1998).
10. J. Markela-Lerenca, N. Illeb, S. Kaisera, P. Fiedlera, C. Mundta, and M. Weisbroda, "Prefrontal-cingulate activation during executive control: Which comes first?," *Brain Res. Cognit. Brain Res.* **18**, 278–287 (2004).
11. M. Rebai, C. Bernard, and J. Lannou, "The Stroop's test evokes a negative brain potential, the N400," *Int. J. Neurosci.* **91**(1–2), 85–94 (1997).
12. M. Liotti, M. G. Woldorff, R. Perez III, and H. S. Mayberg, "An ERP study of the temporal course of the Stroop color-word interference effect," *Neuropsychologia* **38**, 701–711 (2000).
13. M. L. Schroeter, S. Zysset, T. Kupka, F. Kruggel, and D. Y. v. Cramon, "Near-infrared spectroscopy can detect brain activity during a color-word matching Stroop task in an event-related design," *Hum. Brain Mapp* **17**, 61–71 (2002).
14. N. D. Pisapia and T. S. Braver, "A model of dual control mechanisms through anterior cingulate and prefrontal cortex interactions," *Neurocomputing* **69**, 1322–1326 (2006).
15. S. A. Bunge, K. N. Ochsner, J. E. Desmond, G. H. Glover, and J. D. E. Gabrieli, "Prefrontal regions involved in keeping information in and out of mind," *Brain* **124**, 2074–2086 (2001).
16. M. P. Milham, M. T. Banich, and V. Barada, "Competition for priority in processing increases prefrontal cortex's involvement in top-down control: an event-related fMRI study of the stroop task," *Brain Res. Cognit. Brain Res.* **17**(2), 212–222 (2003).
17. H. C. Leung, P. Skudlarski, J. C. Gatenby, B. S. Peterson, and J. C. Gore, "An event-related functional MRI study of the Stroop color word interference task," *Cereb. Cortex* **10**(6), 552–560 (2000).
18. M. T. Banich, M. P. Milham, R. A. Atchley, N. J. Cohen, A. Webb, T. Wszalek, A. F. Kramer, Z. P. Liang, V. Barad, D. Gullett, C. Shah, and C. Brown, "Prefrontal regions play a predominant role in imposing an attentional 'set': evidence from fMIRI," *Brain Res. Cognit. Brain Res.* **10**(1–2), 1–9 (2000).
19. R. P. Kennan, D. Kim, A. Maki, H. Koizumi, and R. T. Constable, "Non-invasive assessment of language lateralization by Transcranial near infrared optical topography and functional MRI," *Hum. Brain Mapp* **16**(3), 183–189 (2002).
20. Y. Hoshi, "Functional near-infrared optical imaging: Utility and limitations in human brain mapping," *Psychophysiology* **40**, 511–520 (2003).
21. F. F. Jöbsis, "Noninvasive infrared monitoring of cerebral and myocardial oxygen suffciency and circulatory parameters," *Science* **198**, 1264–1267 (1977).
22. B. Chance, J. S. Leigh, H. Miyake, D. S. Smith, S. Nioka, R. Greenfeld, M. Finander, K. Kaufmann, W. Levy, M. Young, P. Cohen, H. Yoshioka, and R. Boretsky, "Comparison of time-resolved and -unresolved measurements of deoxyhemoglobin in brain," *Proc. Natl. Acad. Sci. U.S.A.* **88**, 4971–4975 (1988).
23. M. Wolf, M. Ferrari, and V. Quaresima, "Progress of near-infrared spectroscopy and topography for brain and muscle clinical applications," *J. Biomed. Opt.* **12**(6), 062104–062114 (2007).
24. M. Izzetoglu, K. Izzetoglu, S. Bunce, H. Ayaz, A. Devaraj, B. Onaral and K. Pourrezaei, "Functional near-infrared neuroimaging," *IEEE Trans. Neural Syst. Rehabil. Eng.* **13**(2), 153–159 (2005).
25. H. Obrig, R. Wenzel, M. Kohl, Susanne Horst, P. Wobst, J. Steinbrink, F. Thomas, and A. Villringer, "Near-infrared spectroscopy: does it function in functional activation studies of the adult brain?," *Int. J. Psychophysiol* **35**, 125–142 (2000).
26. B. Chance, Q. Luo, S. Nioka, D. C. Alsop, and J. A. Detre, "Optical investigations of physiology: A study of intrinsic and extrinsic biomedical contrast," *Philos. Trans. R. Soc. London, Ser. B* **352**, 707–716 (1997).
27. J. Leon-Carrion, J. Damas-Lopez, J. F. Martin-Rodriguez, J. M. Dominguez-Roldan, F. Murillo-Cabezas, J. Martin, and M. R. Dominguez-Morales, "The hemodynamics of cognitive control: the level of concentration of oxygenated hemoglobin in the superior prefrontal cortex varies as a function of performance in a modified Stroop task," *Behav. Brain Res.* **193**(2), 248–256 (2008).
28. M. Ferrari, L. Mottola, and V. Quaresima, "Principles, techniques, and limitations of near infrared spectroscopy," *Can. J. Appl. Physiol.* **29**(4), 463–487 (2004).
29. Y. A. B. D. Wickramasinghe, P. Rolfe, K. Palmer, S. Watkins, S. A. Spencer, M. Doyle, S. O'Brien, A. Walker, C. Rice, and C. Smallpeice, "Development and clinical evaluation of noninvasive near-infrared monitoring of cerebral oxygenation," *Proc. SPIE* **2085**, 29–37 (1993).
30. A. Villringer and B. Chance, "Non-invasive optical spectroscopy and imaging of human brain function," *Trends Neurosci.* **20**(10), 435–442 (1997).
31. S. G. Horovitz and J. C. Gore, "Simultaneous event-related potential and near-infrared spectroscopic studies of semantic processing," *Hum. Brain Mapp* **22**, 110–115 (2004).
32. H. Shibasaki, "Human brain mapping: Hemodynamic response and electrophysiology," *Clin. Neurophysiol.* **119**(4), 731–743 (2008).
33. C. Bledowski, D. Prvulovic, K. Hoechstetter, M. Scherg, M. Wibral, R. Goebel, and D. E. J. Linden, "Localizing P300 generators in visual target and distractor processing: a combined event-related potential and functional magnetic resonance imaging study," *J. Neurosci.* **24**(42), 9353–9360 (2004).
34. T. Lidaka, A. Matsumoto, K. Haneda, T. Okada, and N. Sadato, "Hemodynamic and electrophysiological relationship involved in human face processing: Evidence from a combined fMRI–ERP study," *Brain Cogn* **60**, 176–186 (2006).
35. G. Gratton, M. R. Goodman-Wood, and M. Fabiani, "Comparison of neuronal and hemodynamic measures of the brain response to visual stimulation: an optical imaging study," *Hum. Brain Mapp* **13**(1), 13–25 (2001).
36. Y. Zheng, Q. Luo, Q. Liu, T. Li, Z. Zhang, and H. Gong, "A portable instrument for brain activity detection based on near-infrared spectroscopy," *Chin. J. Biomed. Eng.* **26**(6), 898–902 (2007).
37. B. Chance, M. Cope, E. Gratton, N. Ramanujam, and B. Tromberg, "Phase measurement of light absorption and scatter in human tissue," *Rev. Sci. Instrum.* **69**(10), 3457–3481 (1998).
38. J. Qiu, Y. Luo, Q. Wang, F. Zhang, and Q. Zhang, "Brain mechanism of Stroop interference effect in Chinese characters," *Brain Res.* **1072**, 186–193 (2006).
39. A. W. MacDonald, J. D. Cohen, V. A. Stenger, and C. S. Carter, "Dissociating the role of the dorsolateral prefrontal and anterior cingulate cortex in cognitive control," *Science* **288**(5472), 1835–1838 (2000).
40. M. Botvinick, L. E. Nystrom, K. Fissell, C. S. Carter, and J. D. Cohen, "Conflict monitoring versus selection-for-action in anterior cingulate cortex," *Nature (London)* **402**(6758), 179–181 (1999).
41. V. van Veen, J. D. Cohen, M. M. Botvinick, V. A. Stenger, and C. S. Carter, "Anterior cingulate cortex, conflict monitoring, and levels of processing," *Neuroimage* **14**(6), 1302–1308 (2001).
42. J. G. Kerns, J. D. Cohen, A. W. MacDonald, R. Y. Cho, V. A. Stenger, and C. S. Carter, "Anterior Cingulate conflict monitoring and adjustments in control," *Science* **303**(5660), 1023–1026 (2004).